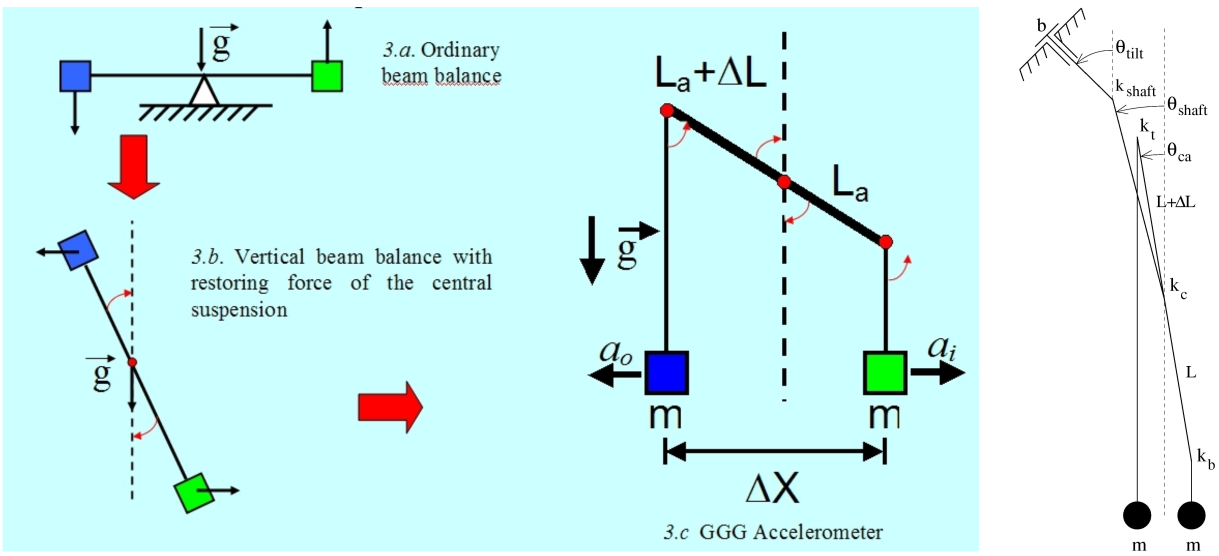

Figure 1: Simplified representation of the GGGonGround balance. On the left side: the GGGonGround accelerometer is designed to be sensitive to differential forces acting in the horizontal plane perpendicular to the spin axis. The two test masses are coupled as in a vertical beam balance. On the right side: the upper part of the shaft, rotating on bearings (b) is tilted by the angle θ_{tilt} by the terrain and bearings tilt noise; the 2D joint k_{shaft} on the shaft attenuates θ_{tilt} so that the lower part of the shaft is tilted by the attenuated angle $\theta_{shaft} = \frac{k_{shaft}}{M_{tot} g L_{shaft}} \theta_{tilt} \ll \theta_{tilt}$ at low frequencies. The coupling arm (ca) equilibrium position corresponding to the shaft tilt is $\theta_{ca} = \frac{k_{ca}}{mgL} \theta_{shaft}$.

Figure 2: In order to isolate the GGonGround rotating accelerometer from terrain and ball bearings noise (tilts and horizontal accelerations) the current design (left side diagram) exploits the attenuation provided at low frequencies by the 2D flexible joint (part 11r) insulating the upper part of the shaft (9r), subject to ground tilts and ball bearings (8) noise, from the lower part (12r), holding the GGonGround differential accelerometer. The isolated part of the shaft (12r) remains in vertical position driven by local gravity. The central image shows the open GGonGround vacuum chamber, shown closed and with thermal insulation in place in the right side image.

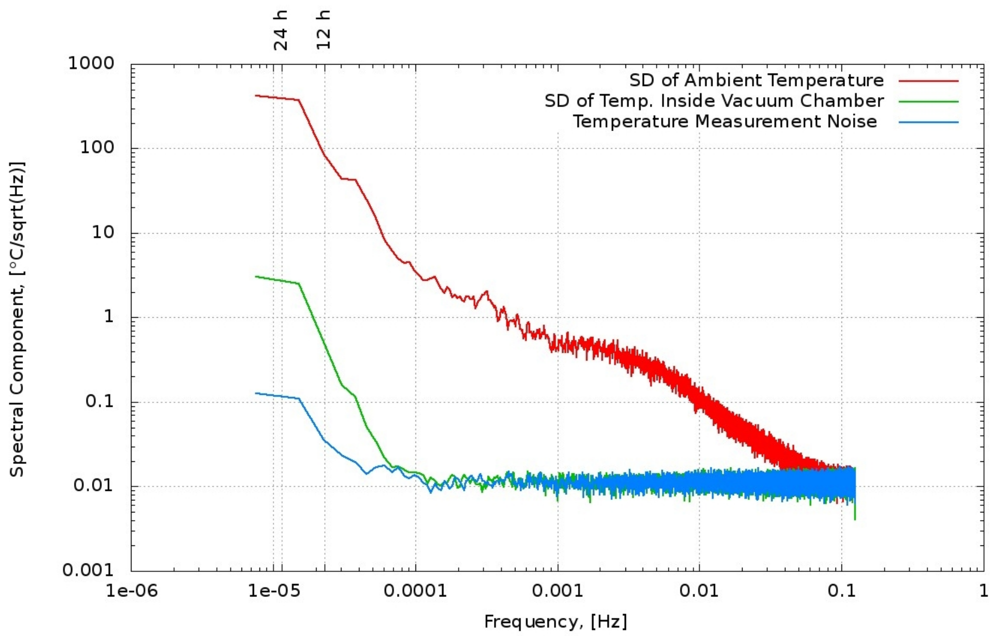

Figure 3: GGonGround temperature stability rely on a PID (Proportional Integral Derivative), heating only, temperature control that acting on the temperature of vacuum chamber walls. Ambient temperature variations (in red) are attenuated inside the vacuum chamber (in green) by about two order of magnitude, limited only by the temperature readout noise at frequencies higher than 10^{-4} Hz.

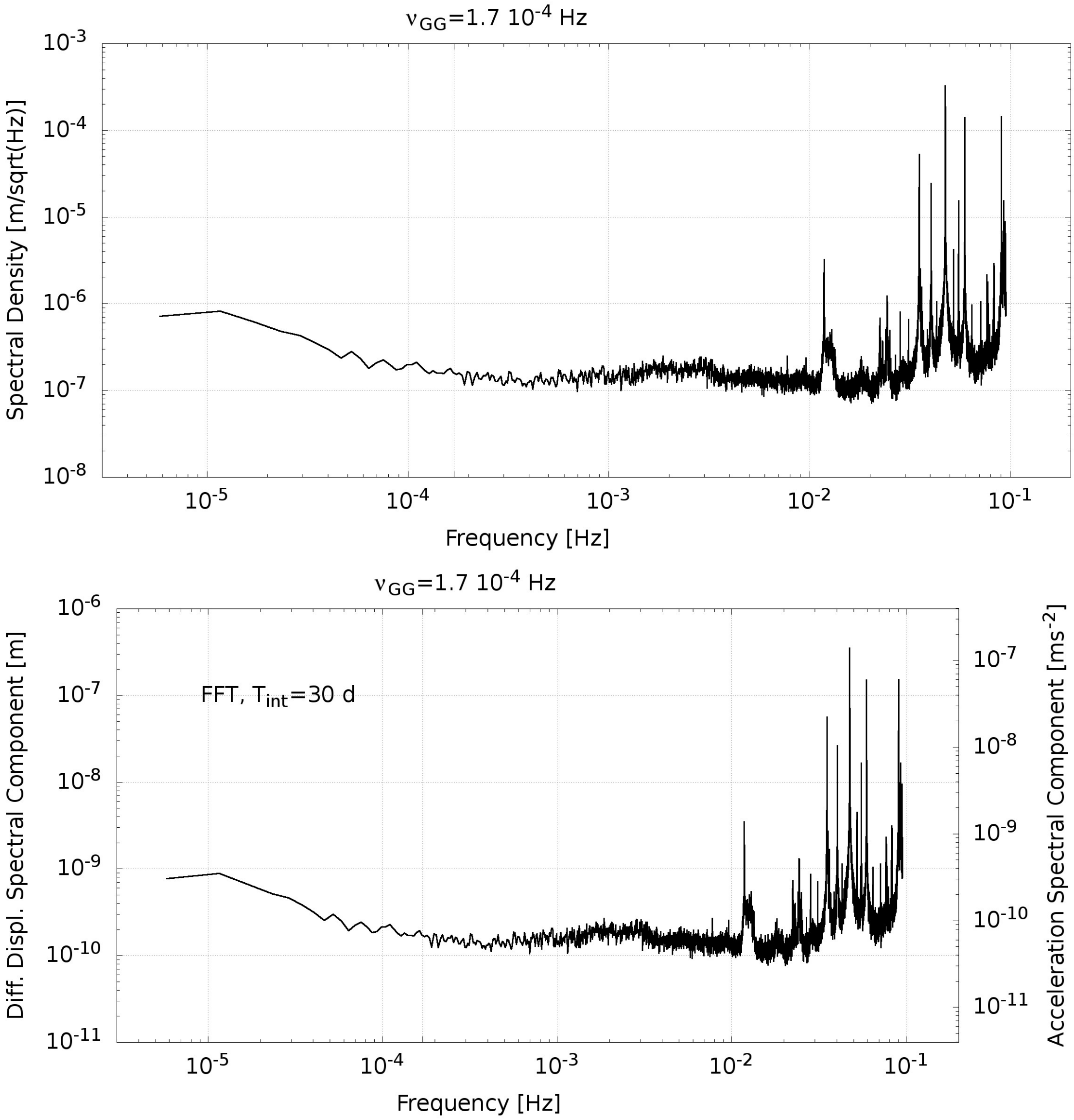

Figure 4: The GGonGround noise performance has been measured from an ongoing run of duration (at time of writing) $T_{\rm meas} \simeq 28$ d. Top plot: Spectral density of the relative displacements of the test cylinders in one direction of the horizontal plane of the lab; the GGonGround differential accelerometer is spinning at $\nu_s = 0.19$ Hz with natural coupling frequency of 0.1 Hz. The measured relative displacement is $\simeq 2 \cdot 10^{-7}\mathrm{m}/\sqrt{\mathrm{Hz}}$ at the frequency $\nu_{\rm GG} \simeq 1.7 \cdot 10^{-4}$ Hz, the orbital frequency relevant for GG in space. Bottom plot: measured relative test masses displacement and acceleration noise integrated over the full run duration (extrapolated to $T_{\rm int} \simeq 30$ d). At $\nu_{\rm GG}$ we measure an integrated differential displacement noise of $\simeq 2 \cdot 10^{-10}$ m and a differential acceleration noise of $\simeq 8 \cdot 10^{-11}$ m/s^2.

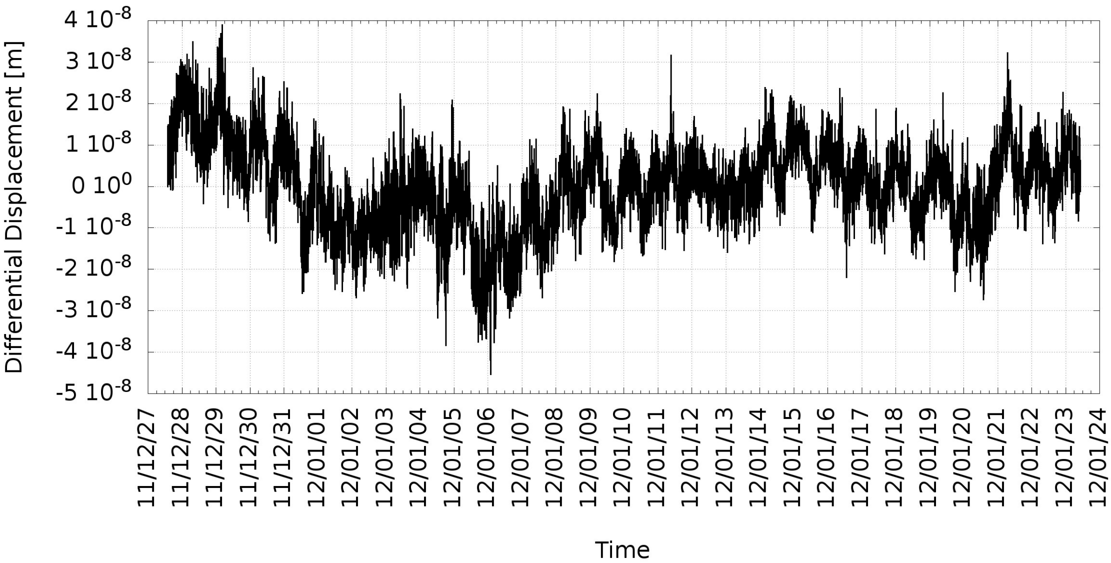

Figure 5: Low frequency component ($\nu_{cut} = 1$ mHz) of the differential displacement between the GGonGround test cylinders in one direction of the lab measured during the (at time of writing) $\mathrm{T_{meas}} \simeq 28$ d ongoing run.